

Fabrication of SnO₂/Reduced Graphene Oxide Nanocomposite Films for Sensing NO₂ Gas at Room-Temperature

Pi-Guey Su*, Ching-Hsuan Wei and Wei-Luen Shiu

Department of Chemistry, Chinese Culture University, Taipei 11114, Taiwan

*Corresponding Author: spg@faculty.pccu.edu.tw

Abstract : *One-pot polyol process was combined with metal organic decomposition (MOD) method to fabricate a room-temperature NO₂ gas sensor based on tin dioxide and reduced graphene oxide (SnO₂/RGO) nanocomposite films. X-ray diffractometry (XRD) and scanning electron microscopy (SEM) were used to analyze the structure and morphology of the fabricated films. The electrical and NO₂ gas-sensing properties of SnO₂ to which various amounts of RGO were added were measured in detail as a function of concentration of NO₂ gas at room temperature, to elucidate the contribution of RGO to the NO₂ gas-sensing capacity. The sensor that was based on a nanocomposite film of SnO₂/RGO exhibited a strong response to low concentrations of NO₂ gas at room temperature, satisfactory linearity and favorable long-term stability.*

Keyword: Tin dioxide (SnO₂); reduced graphene oxide (RGO); nanocomposite film; room-temperature NO₂ sensor.

1. Introduction

NO₂ generated by combustion facilities and automobiles are known to be extremely harmful to the human body and the environment, so highly sensitive detection is needed for monitoring NO₂ gas. Metal oxides are well known to be effective in detecting various gases with enough sensitivity. Tin dioxide (SnO₂), as oxygen-deficient n-type semiconductor with a wide bandgap ($E_g = 3.6$ eV), much effort has been made to elucidate their ability to detect various toxic and flammable gases [1-3]. According to reports, the SnO₂ sensors operate only at high temperatures, such as 200~500°C. Accordingly, the development of SnO₂ sensors that can operate at lower temperatures, with high sensitivity and low production cost has attracted much attention [4,5].

Graphene consists of a two-dimensional (2D) array of carbon atoms that are covalently connected via sp² bonds to form a honeycomb sheet [6]. Graphene oxide (GO) sheets have recently become attractive as possible intermediates in the manufacture of graphene [7]. GO can be chemically or thermally reduced to conductive reduced GO (RGO) [8]. Many methods have been used to prepare metal oxide/graphene composite materials, including the hydro/solvothermal method, solution mixing method, the in-situ growth method and the photoreduction method, all of which have their own advantages and particular conditions of application [9-11]. Among these methods, hydro/solvothermal method is the most widely used to prepare metal oxide/graphene composite because chemical bonds form between metal oxides and graphene, which can improve the electric properties of the composite over those of the same metal oxides or graphene alone. Recently, composite films that are

based on SnO₂ nanopowders and graphene have been reported to be as new gas-sensitive materials to reduce further the operating temperature and to improve the sensitivity of sensors based on these materials [12,13]. Neri *et al.* fabricated SnO₂/graphene nanocomposites using the one-pot microwave-assisted non-aqueous sol-gel method for sensing NO₂ [12]. Zhang *et al.* fabricated a more rapidly responding NO₂ gas sensor based on SnO₂ nanoparticles/graphene nanocomposites that were made by the hydrothermal treatment of aqueous dispersion of GO in the presence of Sn salts [13]. The sensing characteristics of these SnO₂/graphene-based NO₂ gas sensors depend on their microstructure, which are determined by their fabrication process. Most NO₂ gas sensors have been fabricated by synthesizing graphene that is decorated with SnO₂ nanomaterial and drop-coating it on a substrate. In this work, SnO₂/RGO nanocomposite films were fabricated by combining the one-pot process with the metal organic decomposition (MOD) method. These films have the advantages of being highly effective, inexpensive and suitable for industrial for mass production. The structural characteristics of the SnO₂/RGO nanocomposite films were investigated by X-ray diffraction (XRD). The surface characteristics of the SnO₂/RGO nanocomposite films were observed using scanning electron microscopy (SEM). The NO₂ sensing performance of SnO₂/RGO nanocomposite films with various amounts of the RGO loaded into the SnO₂ matrix was studied as a function of concentration of NO₂ gas at room temperature. Differences in the composition and microstructure were adopted to explain the effect of adding RGO on the sensing mechanism of the SnO₂/RGO nanocomposite films.

2. Experimental

2.1 Preparation of RGO in glycerol solution

GO was prepared from natural graphite by a modified Hummers method [14]. Briefly, 0.5 g graphite powder was reacted with a mixture of 2 g NaNO₃, 12 mL concentrated H₂SO₄ and 3 g KMnO₄; then 40 mL deionized water (DIW) and 10 mL H₂O₂ (30%) were added. The resultant mixture was filtered and washed with DIW by centrifuging until the solution attained a pH of 6, and was then sonicated to form a stable suspension of GO in aqueous media. The resulting aqueous GO solution had a concentration of 0.85 mg/mL. The GO was reduced to form RGO in glycerol solution that was prepared as follows: the required amounts of GO were added to 10 g of glycerol and the resultant solution was heated to 190°C for 1 h with vigorous magnetic stirring. The solution was continuously stirred until a stable suspension was obtained.

2.2 Fabrication of gas sensors based on SnO₂/RGO nanocomposite films

An organometallic solution (Sn [OOCCH (C₂H₅) C₄H₉]₂,aq.; Tin (II) 2-ethylhexanoate ~ 90 % in 2-ethylhexanoic acid) was used as the precursor in fabricating the gas-sensing material (SnO₂). The organometallic solution was obtained from Strem Chemicals Inc. The solution includes about 28wt% Sn. The SnO₂/RGO nanocomposite films were fabricated as follows: the Tin (II) 2-ethylhexanoate was added and dispersed in the precursor solutions of RGO by ultrasonic vibration for about 2 hours to obtain the well-mixed suspensions. Then, the suspensions were coated onto the surfaces of the Au comb electrodes and the Al₂O₃ substrate by spin coating. The spinning was at 1000 rpm/min and the period of coating was 20 seconds. Thereafter, the coating layers were heated in air using an infra-red dryer at approximately 150°C for 30 minutes, to evaporate the solvents in the coating layers. Finally, the coating layers were sintered at an MOD temperature of 500°C for 4 h, to decompose the coating materials, and obtain SnO₂/RGO nanocomposite films. This sintering process yielded sensing films of appropriate mechanical strength and also conferred thermal stability, as shown in Fig. 1.

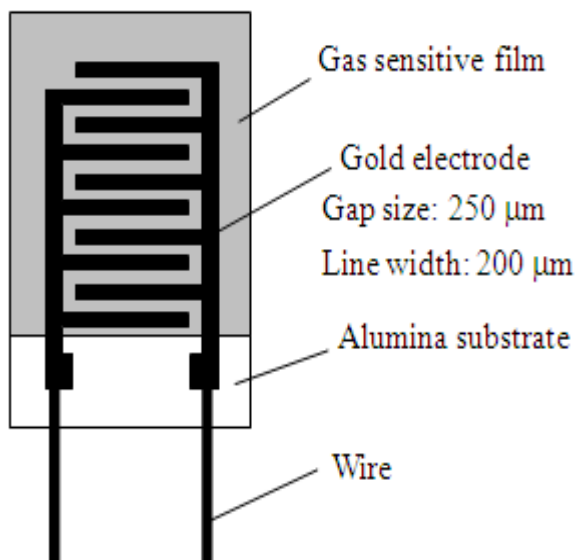


Fig. 1 Structure of NO₂ gas sensor.

2.3 Instruments and analysis

The surface microstructure of the SnO₂/RGO nanocomposite films coated on an alumina substrate was investigated using a field emission scanning electron microscope (FEI company, Nova NanoSEM™ 230). The XRD powder pattern of the SnO₂ film and SnO₂/RGO nanocomposite films were measured using Cu K_α radiation (Shimadzu, Lab XRD-6000). The electrical and sensing characteristics were measured using a static state system at room temperature, as shown in Fig. 2. Each sensor was connected in series with a load resistor and a fixed 5V tension (DC mode) was continuously supplied to the sensor circuit from a power supply (GW, PST-3202). The resistance of the sensor was determined from the voltage at the ends of the

load resistor using a DAQ device (NI, USB-6218) in various concentrations of gas. The concentration for standard NO₂ and NH₃ gases were 100,000 and 1000. The required various gas concentrations were produced by diluting the known volume of standard gas with dry air and then were injected into the chamber. The desired various gas concentrations were measured using a calibrated gas sensor system (Dräger, MiniWarn). The interfering experiment was performed by measuring the resistance of the sensor exposure to NH₃ and H₂O gases, respectively. The volume of the chamber is 18 liters. The gas inside the chamber was uniformly distributed using a fan. After some time, the chamber was purged with air and the experiment was repeated for another cycles. All experiments were performed at room temperature, which was about 23.0 ± 1.5°C and the relative humidity was 40% RH. The sensor response (S) was calculated by the following equation:

$$S(\%) = \frac{(R_{gas} - R_{air})}{R_{air}} \times 100\% = \frac{(\Delta R)}{R_{air}} \times 100\%$$

(1)

where R_{gas} and R_{air} are the electrical resistances of the sensor in the tested gas and air, respectively.

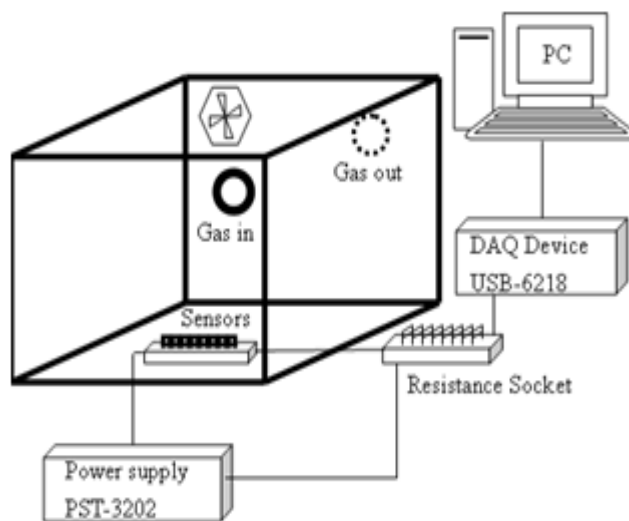


Fig. 2 Measurement system for testing gas sensors

3. Results and discussion

3.1 Morphology observations

Figure 3 presents SEM images of the SnO₂ film and the SnO₂/RGO nanocomposite films that were formed by MOD at 500°C. The SnO₂ film exhibited a flat and needle-shaped surface (Fig. 3(a)). When the RGO was added into the SnO₂ matrix, the surface of the SnO₂/RGO nanocomposite film exhibited a flat covered with granules. Moreover, no naked RGO was present on the surface of the intentionally fractured SnO₂/RGO nanocomposite film, even when the amount of added RGO was increased to 0.05 g. The RGO were embedded in the SnO₂ matrix and uniformly dispersed therein (Fig. 3(b)).

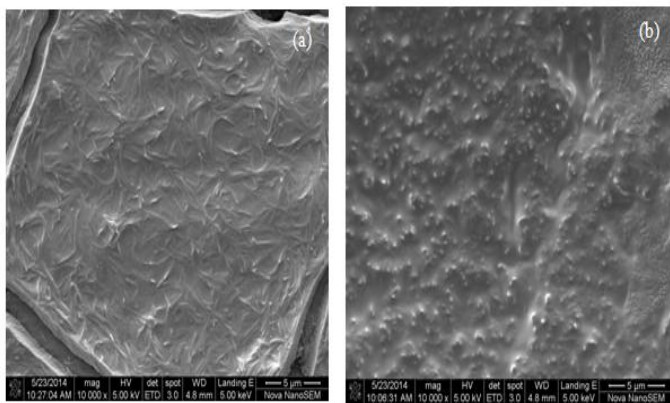


Fig. 3 FE-SEM images of (a) SnO₂ film and (b) SnO₂/RGO nanocomposite film that were fabricated by one-pot process and MOD at 500°C.

3.2 XRD characterization

Figure 4 shows the XRD spectra of the SnO₂ film and SnO₂/RGO nanocomposite films that were prepared by the combined one-pot process and MOD method. The XRD patterns of SnO₂ film show three main peaks at $2\theta = 26.56, 33.82, 51.50$ and 65.42° , which are identified as corresponding to (1 0 0), (1 0 1), (2 1 1) and (1 1 2) planes of tetragonal rutile SnO₂, indicating the formation of SnO₂ crystals. For the SnO₂/RGO nanocomposite, the XRD patterns showed no appreciable difference between the orientations and phases of SnO₂ and SnO₂/RGO samples, probably due to the reduction of GO by glycerol [15] or RGO was embedded in the SnO₂ matrix and so could not be easily detected by X-ray diffraction.

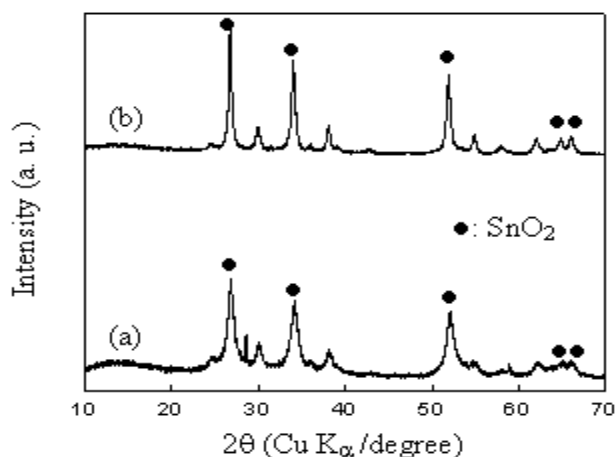


Fig. 4 XRD patterns of (a): SnO₂ film and SnO₂/RGO nanocomposite films that were fabricated by one-pot process and MOD at 500°C.

3.3 Gas sensing characteristics of SnO₂ film and SnO₂/RGO nanocomposite films

Figure 5 plots the responses of the sensors that were based on SnO₂ film and SnO₂/RGO nanocomposite films that were prepared using various amounts of RGO, to various concentrations of NO₂ gas at room temperature. Clearly, the responses (S) of the sensors that were made of the SnO₂/RGO nanocomposite films were significantly stronger than that of the sensor that was made of the pure SnO₂ film. The NO₂ gas sensor

that was made of the SnO₂/RGO nanocomposite film that was doped with 0.01 g of RGO was chosen to study further its other gas sensing characteristics because this sensor exhibited the highest response.

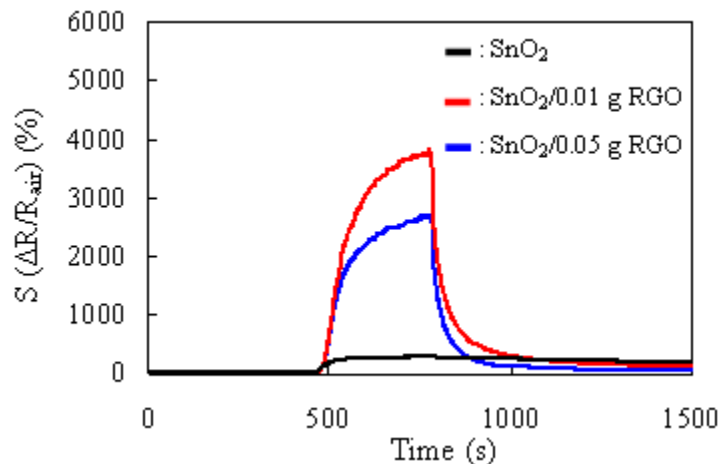


Fig. 5 Response (S) of NO₂ gas sensors based on SnO₂ film and SnO₂/RGO nanocomposite films that were prepared by one-pot process and MOD at 500°C for 4 h with various amounts of added RGO in response to 5 ppm NO₂ gas.

Figure 6 plots the response (S) as a function of concentration of NO₂ gas for the sensor that was made of the SnO₂/0.01 g RGO

nanocomposite film. The sensitivity ($\frac{\Delta S}{\Delta C}$) is determined from the slopes of the plots of response vs. gas concentration.

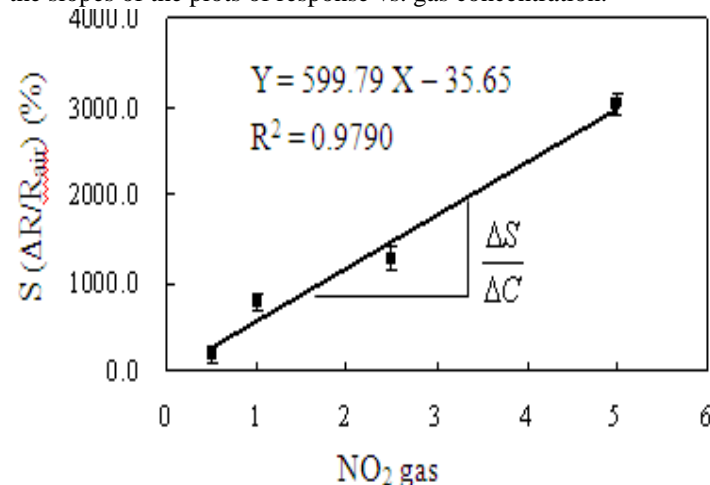


Fig. 6 Linear dependence of response of NO₂ gas sensor based on SnO₂/0.01 g RGO nanocomposite film on concentration of

NO₂ gas at room temperature. Sensitivity ($\frac{\Delta S}{\Delta C}$) is determined

from the slope of the linear curve.

The response time is defined as the time required for the sensor to reach 90% of the maximum change in resistance following exposure to a given NO₂ gas. The recovery time is defined as the time required for the sensor to recover 90% of the decrease in resistance after the sensor is exposed to a dry gas. The response and recovery times of the NO₂ gas sensor were 4.9 and

6.0 min, respectively, at a testing concentration of NO₂ of 5 ppm. Figure 7 plots the results concerning the interfering effects of NH₃ gas on the NO₂ gas sensor. NH₃ gas may be regarded as having unobvious interference effects with NO₂ at a testing NO₂ concentration of 2.5 ppm.

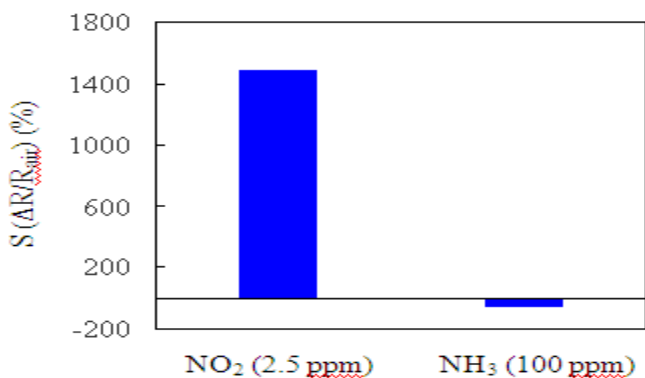


Fig. 7 Response (S) of NO₂ gas sensors based on SnO₂/0.01 gRGO nanocomposite film to interfering gas NH₃. Figure 8 plots the effect of ambient humidity on the response (S) of the NO₂ gas sensor at a testing NO₂ concentration of 5 ppm. The response (S) of the NO₂ gas sensor decreased as the ambient humidity increased, because the physisorbed water occupied the active sites of the sensing materials.

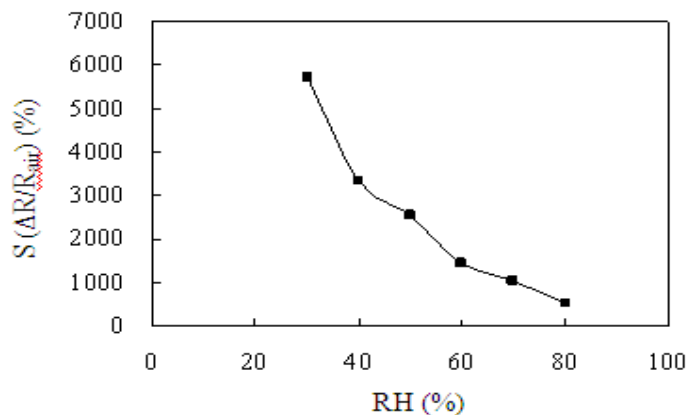


Fig. 8 Effect of ambient humidity on response of the NO₂ gas sensor based on WO₃/0.01 g RGO nanocomposite film to 5 ppm of NO₂ gas at room temperature. Figure 9 plots the long-term stability. The response (S) of the NO₂ gas sensor did not significantly vary for at least 50 days in a testing NO₂ concentration of 2.5 ppm.

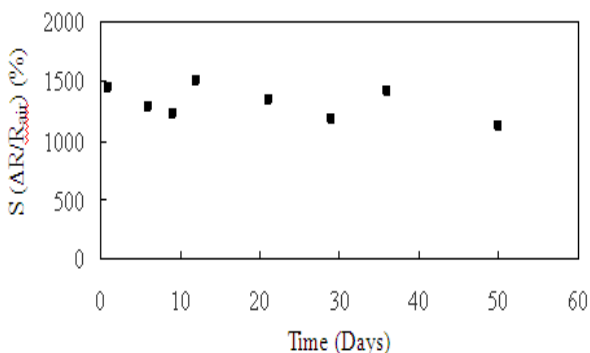


Fig. 9 Long-term stability of response of the NO₂ gas sensor based on SnO₂/0.01 g RGO nanocomposite film in 2.5 ppm of NO₂.

Table 1 compares the performance of NO₂ gas sensor that is developed herein with that of the NO₂ gas sensor that was based on the RGO/SnO₂ nanocomposite sensing materials. The response of the NO₂ gas sensor that is developed herein was higher than of those reported literatures.

Table 1 Comparison of performance of NO₂ gas sensor developed herein with the literatures.

Sensing material	Fabrication method	Response (%)	References
RGO was embedded in the SnO ₂ matrix	one-pot process combined with MOD	1271 ^a	This work
SnO ₂ nanoparticles decorated on the surface of graphene	one-pot microwave-assisted non-aqueous sol-gel	900 ^b	[12]
SnO ₂ nanoparticles decorated on the surface of graphene	hydrothermal	75 ^c	[13]

^a The sensor in response to 2.5 ppm NO₂ gas at room temperature.

^b The sensor in response to 8 ppm NO₂ gas at 100°C.

^c The sensor in response to 5 ppm NO₂ gas at 100°C.

4. Conclusion

A new SnO₂/RGO nanocomposite gas sensor was developed herein with high sensitivity and favorable recovery properties in detecting NO₂ gas at room temperature. The new SnO₂/RGO nanocomposite gas sensor solves the problems of conventional SnO₂ sensors that cannot detect NO₂ gas at room temperature. The preparation of the SnO₂/RGO nanocomposite sensor was simple. The fabrication procedure involves the heat treatment of SnO₂ with RGO, which are initially dispersed in an organometallic solution. This new gas sensor will be adapted in the near future to a NO_x gas sensor that uses less power than current NO_x gas sensors.

This work found that the sensitivity of the new SnO₂/RGO nanocomposite sensor to NO₂ increases dramatically if only a few RGO are added as dopants to the SnO₂ substrate.

The NO₂ gas sensor that was based on a SnO₂/RGO film exhibited very sensitive with acceptable linearity ($Y = 599.79 X - 35.5$; $R^2=0.9790$) between 0.5 and 5 ppm, good reversibility and long-term stability (at least 50 days) when used at room temperature. NH₃ gas may be regarded as having unobvious

interference effects with NO₂ at a testing NO₂ concentration of 2.5 ppm. Ambient humidity significantly affected the NO₂ gas sensor.

Acknowledgement

The authors thank the Ministry of Science and Technology (grant no. MOST 103-2113-M-034-001) of Taiwan for support.

REFERENCES

- i. Fang, G. J., Liu, Z. L., Ji, X. D., Wang, H. Z., Yao, K. L. 1999. Novel NO₂-Sensing properties of sol-gel-derived SnO₂-(Y₂O₃) thin films, *J. Mater. Sci. Lett.* 18, 639-641.
- ii. Promsong, L., Sriyudthsak, M. 1995. Thin tin-oxide film alcohol-gas sensor, *Sens. Actuators B* 24-25, 504-506.
- iii. Barsan, N., Schweizer-Berberich, M., Göpel, W. 1999. Fundamental and practical aspects in the design of nanoscaled SnO₂ gas sensors: a status report, *Fresenius J. Anal. Chem.* 365, 287-304.
- iv. Niranjana, R. S., Chaudhary, V. A., Mulla, I. S. 2002. A novel hydrogen sulfide room temperature sensor based on copper nanocluster functionalized tin oxide thin films, *Sens. Actuators B* 85, 26-32.
- v. Anothainart, K. 2003. Light enhanced NO₂ gas sensing with tin oxide at room temperature: Conductance and work function measurements, *Sens. Actuators B* 93, 580-584.
- vi. Novoselov, K. S., Geim, A. K., Morozov, S. V., Jiang, D., Zhang, Y., Dubonos, S. V., Grigorieva, I. V., Firsov, A. A. 2004. Electric field effect in atomically thin carbon films, *Science* 306, 666-669.
- vii. Daniela, C., Marcano, V. D., Kosynkin, J. M., Berlin, J. M., Sinitskii, A., Sun, Z., Slesarev, A., Alemany, L. B., Lu, W., Tour, M. J. M. 2010. Improved synthesis of graphene oxide, *Nano* 4, 4806-4814.
- viii. Pei, S. F., Cheng, H. M. 2012. The reduction of graphene oxide, *Carbon* 50, 3210-3228.
- ix. Chen, J., Shi, J., Wang, X., Cui, H., Fu, M. 2013. Recent progress in the preparation and application of semiconductor/graphene composite photocatalysts, *Chin. J. Catal.* 34, 621-640.
- x. Si, Y., Samulski, E. T. 2008. Exfoliated graphene separated by platinum nanoparticles, *Chem. Mater.* 20, 6792-6797.
- xi. Wu, T. S., Liu, S., Luo, Y. L., Lu, W. B., Wang, L., Sun, X. P. 2011. Surface plasmon resonance-induced visible light photocatalytic reduction of graphene oxide: Using Ag nanoparticles as a plasmonic photocatalyst, *Nanoscale* 3, 2142-2144.
- xii. Neria, G., Leonardi, S. G., Latino, M., Donato, N., Baek, S., Conte, D. E., Russo, P. A., Pinna, N. 2013. Sensing behavior of SnO₂/reduced graphene oxide nanocomposites toward NO₂, *Sens. Actuators B* 179, 61-68.
- xiii. Zhang, H., Feng, J., Fei, T., Liu, S., Zhang, T. 2014. SnO₂ nanoparticles-reduced graphene oxide nanocomposites for NO₂ sensing at low operating temperature, *Sens. Actuators B* 190, 472-478.
- xiv. Hummers, W. S., Offeman, R. E. 1958. Preparation of graphitic oxide, *J. Am. Chem. Soc.* 80, 1339.
- xv. Paek, S. M., Yoo, E., Honma, I. 2009. Enhanced cyclic performance and lithium storage capacity of SnO₂/graphene nanoporous electrodes with three-dimensionally delaminated flexible structure, *Nano Lett.* 9, 72-75.